XeF* and XeCl* Formation in Low-Pressure Tesla Coil Discharges

D. J. Wren,[†] **D. W. Setser,*** **and J. K. Ku**

Department of Chemistry, Kansas State University, Manhatten, Kansas 66506 *(Received: April 15, 1981; In Final Form: August 6, 1981)*

The XeCl* and XeF* emission spectra have been studied from mixtures of Xe with HCl, Cl_2, CCl_4, NF_3, BF_3, C_2F_6, and SF_6 in a tesla-coil-driven discharge. The XeX* emission spectra were recorded at pressures below 0.75 torr for all reagents except BF_3 and C_2F_6, which did not give XeF* emission. Low-pressure pulsed dc discharge experiments in Xe/Cl_2 and Xe/HCl mixtures gave XeCl* emission spectra very similar to those observed from the tesla-driven discharge. Computer simulations of the XeCl(B–X) spectra from discharges of Xe with Cl_2, CCl_4, and HCl provide an estimate for the XeCl(B) vibrational distributions. Since Xe($^3P_2$) and Xe($^3P_1$) reacting with HCl and SF_6 do not give XeX*, the observation of XeX* from these two reagents requires the reactions of Xe Rydberg states or recombination of Xe^+ and Cl^- or F^- ions. Arguments based upon XeCl* and XeF* vibrational and electronic state populations and the time dependence of the emission suggest that Rydberg state reactions are the dominant mechanism contributing to the XeX* excitation from the low-pressure discharge of Xe/HCl and Xe/SF_6 mixtures.

Introduction

The rare gas halide state distributions resulting from reactions of excited state rare gas atoms with halogen-containing donor molecules are of interest as state-to-state processes, as well as being of importance for modeling rare gas halide lasers. The rare gas precursor states can be divided into three broad classes, the four states of the first excited manifold, Rg(np^5, $(n + 1)$s), the low-energy Rydberg states, Rg**, and the Rg^+ ion. Low Rydberg states are defined here to be states in the general energy range of the Rg(np^5, $(n + 2)$p) manifold. The reactions of the lower energy metastable ($(n + 1)s[3/2]_2$) and resonance ($(n + 1)s[3/2]_1$) states of Kr and Xe have been isolated and characterized.[1-5] For the same donor the halide product state distributions for the two different states are similar.[4,5] Much less attention has been given to the monatomic ions and the low-lying Rydberg states, especially at low pressure where the rare gas halide product state distributions can be observed. Other possible rare gas halide formation processes include reactions of rare gas excimers,[6] rare gas dimer ions,[7] and excited states of the halogen molecules.[8]

Tellinghuisen and co-workers[9,10] have studied the rare gas halide spectra using a tesla coil as an excitation source. This excitation source has the advantage of low cost and high emission intensity, but the disadvantage common to most discharge sources of being very indiscriminate with respect to excitation mechanism. The tesla coil generates a low current discharge with voltages as high as 50 kV at the spark electrode; the plasma is composed of ions, metastable atoms, and higher excited state rare gas atoms. Comparison of Tellinghuisen's work with the Xe($6s[3/2]_1$ and $[3/2]_2$) studies[1-5] of our laboratory showed that the tesla discharge can generate *strong* XeX* emission from donor molecules which have low branching fractions of XeX* formation from reaction with the Xe($[3/2]_1$ or $[3/2]_2$) states. The four lower energy rare gas atom states are usually identified as $^3P_2$, $^3P_1$, $^3P_0$, and $^1P_1$ and this notation will be used hereafter. Tellinghuisen's work suggests that either ionic or Rg** reactions are important in the discharge. Therefore, we have recorded low-pressure tesla discharge XeX* excitation spectra with emphasis on donor molecules with low branching fraction for XeX* formation by reaction with Xe($^3P_1$ or $^3P_2$). Spectra from Cl_2, HCl, CCl_4, SF_6, NF_3, C_2F_6, and BF_3 were recorded at total pressures between 0.1 and 0.7 torr. Experiments also were done with a low-pressure pulsed dc discharge for the same type of mixtures used for tesla coil excitation. At the lowest pressure, the XeX** molecules are not vibrationally relaxed and simulation of the spectra can be used to assign vibrational distributions, which can be compared to those observed for Xe($^3P_2$) reactions.[3,11] These distributions can help to identify the XeCl* and XeF* formation process in the discharge.

Time-resolved measurements of the Xe** and XeX* emission intensities were made for excitation by both the tesla and pulsed dc discharge. The spectra and decay times for both excitation methods were very similar for the same gas mixtures and pressures. Thus, the XeX* excitation mechanisms in both discharges presumably are the same.

For C_2F_6 and BF_3 no XeF* emission was observed. However, all other reagents, including HCl and SF_6, which do not yield XeX* by reaction of Xe($^3P_{1,2}$) atoms, gave strong XeX* emission. All of the reagents which yield XeX* spectra have electron attachment thresholds below 0.7 eV; whereas, C_2F_6 and BF_3 attach electrons with energies of 2.0 and 10.4 eV, respectively, which may correlate with their difficulty in formation of XeF*. Nighan and

---

[†] Atomic Energy of Canada, Whiteshell Nuclear Research Station, Pinawa, Manitoba ROE IL0, Canada.

(1) J. E. Velazco, J. H. Kolts, and D. W. Setser, *J. Chem. Phys.* **65**, 3468 (1976).

(2) J. H. Kolts, J. E. Velazco, and D. W. Setser, *J. Chem. Phys.*, **69**, 4357 (1978).

(3) (a) J. H. Kolts, J. E. Velazco, and D. W. Setser, *J. Chem. Phys.*, 71, 1247 (1979); (b) K. Tamagake, J. H. Kolts, and D. W. Setser, *J. Chem. Phys.*, 71, 1264 (1979); (c) K. Tamagake, D. W. Setser, and J. H. Kolts, *J. Chem. Phys.*, 74, 4286 (1981).

(4) (a) D. W. Setser, T. D. Dreiling, H. C. Brashears, Jr., and J. H. Kolts, *Faraday Discuss., Chem. Soc.*, **67**, 1255 (1979); (b) D. W. Setser, H. C. Brashears, and T. D. Dreilings, *J. Phys. (Paris) C3*, 41, 195 (1980).

(5) H. C. Brashears, Jr., and D. W. Setser, *J. Phys. Chem.* **84**, 224 (1980).

(6) G. P. Quigley and W. M. Hughes, *Appl. Phys. Lett.*, **32**, 649 (1978).

(7) (a) D. Kligler, D. Pritchard, W. K. Bischel, and C. K. Rhodes, *J. Appl. Phys.*, **49**, 2219 (1978); (b) W. K. Bischel, J. Bokor, D. J. Kligler, and C. K. Rhodes, *IEEE J. Quant. Electon, QE15*, 380 (1979).

(8) (a) M. C. Castex, J. Le Calvé, D. Haaks, B. Jordan, and G. Zimmer, *Chem. Phys. Lett.*, **70**, 106 (1980); (b) D. J. Ehrlich and R. M. Osgood, Jr., *J. Chem. Phys.*, **73**, 3038 (1980).

(9) (a) M. R. McKeever, A. Sur, A. K. Hui, and J. Tellinghuisen, *Rev. Sci. Instrum.*, **50**, 1136 (1979); (b) A. K. Hui, M. R. McKeever, and J. Tellinghuisen, *J. Quant. Spectrosc. Radiat. Transfer*, **21**, 387 (1979).

(10) J. Tellinghuisen and M. R. McKeever, *Chem. Phys. Lett.*, **72**, 94 (1980).

(11) K. Tamagake and D. W. Setser, *J. Chem. Phys.*, **67**, 4370 (1977).

0022-3654/82/2086-0284$01.25/0

Brown[12] have suggested that $Xe^+ + Cl^-$ three-body recombination is the main formation process in lasers operating with a Ne/Xe/HCl high-pressure gas mixture. However, kinetic analysis of our low-pressure experiments tends to rule out the ion recombination mechanism and XeCl* and XeF* most likely are formed by direct reaction of low-energy Rydberg-state Xe atoms with HCl and SF_6, respectively. The Rydberg pathway also augments XeCl* and XeF* formation for reagents that react with Xe(6s) atoms to give XeCl* or XeF*.

Experimental Section

The reactions were studied in a Pyrex flow tube (10 cm long × 8 mm i.d.) fitted with S1-UV quartz windows. The reactant gases were premixed 10 cm upstream of the entrance valve and the partial pressures were measured in the flow tube by a differential pressure transducer. The flow rate through the tube was controlled by a teflon regulating valve on the exit line. Typical flow rates for 0.1 torr were 3 μmol/min. A discharge within the flow tube was struck by a heavy-duty tesla coil (Sargent Welch, Model BD-20) with resonance frequency of 4–5 MHz and 120-Hz repetition rate contacting the tube ~1 cm from the front window. For total pressures less than 1 torr, the discharge extended out the arms of the flow tube. Originally we used a static cell, but the fluorescence was not stable for pressure below a few torr. The emission intensity reached a maximum after ~2 min and then decayed with a time constant of ~1 min, presumably because of consumption of the reactant by the discharge process. Changing to a flow cell allowed stable spectra to be obtained for pressures > 0.1 torr.

The spectra were observed with a McPherson 0.3-m monochromator equipped with a 1200 groove/mm grating blazed at 300 nm. Photons were detected by an RCA 31034 photomultiplier cooled to −20 °C in an rf-shielded Products for Research housing. The photomultiplier current was measured by Keithly 417 electrometer and the signal recorded by a PDP-8 computer, which was also interfaced to the wavelength drive of the monochromator. The electrometer input was damped to remove the 120 cycle oscillations in the signal caused by the oscillation of the tesla field. All spectra shown here have been corrected for the wavelength response to the light detection system.

The time dependence of the emission intensity was measured by replacing the electrometer with a Biomation transient digitizer. The photomultiplier current was passed directly to the 50-Ω input of the Biomation via 1 m of coaxial cable. The signal acquisition was triggered from the rf noise generated by the tesla coil discharge.[9] An antenna formed by a 1-m coil of copper wire was connected directly to the 50-Ω trigger input of the Biomation. The antenna signal was sufficient to trigger the Biomation, but the inherent erratic nature of the tesla discharge made adjustment of the trigger level and the resultant triggering imprecise, especially for acquisition with a large sampling time. The Biomation was interfaced to a PDP 11/34 computer which performed the necessary signal averaging. Typically 1000 scans were acquired and averaged to obtain an intensity waveform.

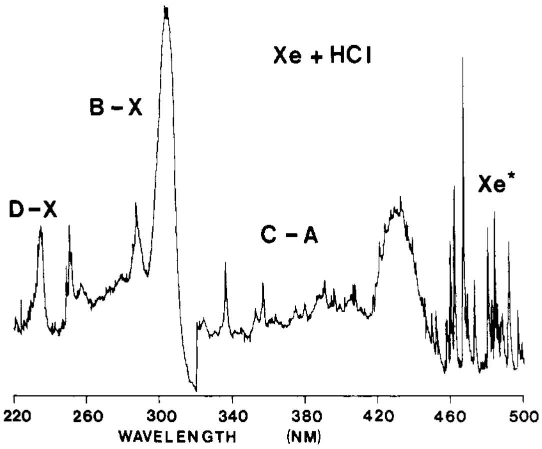

Figure 1. Spectrum from HCl/Xe discharge at 0.2-nm resolution: P_{Xe} = 0.12 torr and P_{HCl} = 0.04 torr. The XeCl* bands are labeled. The band at 250 nm is the Cl_2(E–B) transition and the bands at 287.7, 337.1, and 358.0 nm are from H_2O and N_2 impurities. The lines beyond 460 nm are Xe($5p^57p$–$5p^56s$) transitions. These is a factor of 3 change in scale at ~320 nm.

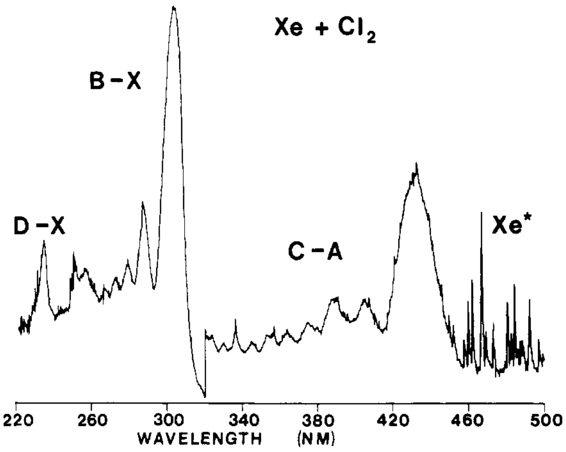

Figure 2. Spectrum from Cl_2/Xe discharge at 0.2-nm resolution: P_{Xe} = 0.12 torr and P_{Cl_2} = 0.04 torr. See Figure 1 for further description.

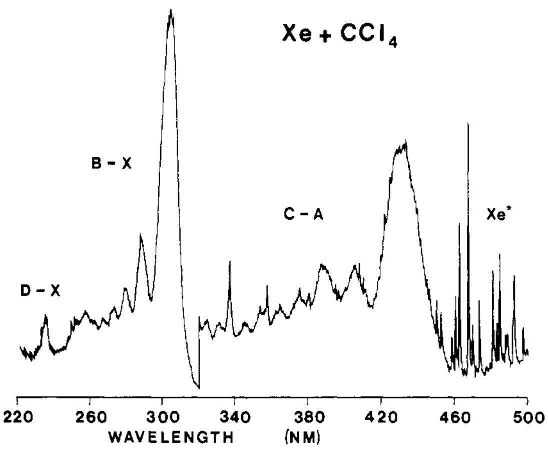

Figure 3. Spectrum from CCl_4/Xe discharge at 0.3-nm resolution: P_{Xe} = 0.20 torr and P_{CCl_4} = 0.01 torr. See Figure 1 for further description.

Measurements of XeCl* and XeX* emission intensities also were made during and in the afterglow of a pulsed dc discharge.[13] The design and operation of the discharge is discussed by Nguyen and Sadeghi;[13a] the discharge parameters are more carefully controlled with this device than in a tesla discharge. In the present work the pulsed discharge experiments were done only to confirm observations from the low-pressure tesla discharge experiments. The discharge cell used tantalum electrodes placed in side arms attached to the reaction cell. Otherwise the cell dimensions were the same as the one used for the tesla experiment. Observations were made by viewing the cell end-on.

---

[12] W. L. Nighan and R. T. Brown, *Appl. Phys. Lett.*, **36**, 498 (1980).

[13] (a) T. D. Nguyen and N. Sadeghi, *Phys. Rev. A*, **18**, 1388 (1978); (b) G. Inoue, D. W. Setser, and N. Sadeghi, *J. Chem. Phys.*, submitted for publication.

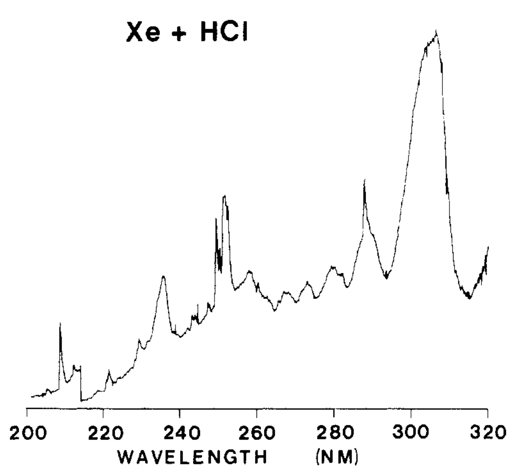

Figure 4. The short wavelength XeCl(B–X) and XeCl(D–X) spectrum from the HCl/Xe discharge showing the short wavelength cutoff at ~200 nm: P_{Xe} = 0.11 torr and P_{HCl} = 0.01 torr. This spectrum was obtained with 0.3-m monochromator but with VUV photomultiplier tube and grating.

Results

A. Xe + RCl. The XeCl* emission spectra observed from HCl, Cl_2, and CCl_4 are shown in Figures 1–3. All three spectra show the D–X, B–X, and C–A bands of XeCl, as well as Xe lines above 450 nm. The narrow features at 287.7, 337.1, and 358.0 nm are OH and N_2 emission from water and nitrogen impurities. The feature at 250–260 nm is the Cl_2(E–B) band. The very narrow spikes (both positive and negative) throughout the spectrum are due to spurious noise picked up by the computer from the tesla discharge. The most notable aspect of Figures 1–3 is the close similarity of the three spectra in spite of the differing bond energies and natures of the Cl_2^-, HCl^-, and CCl_4^- ions, which are crucial factors in governing the energy disposal from Xe($^3P_{2,1}$) reactions.[3,4]

The XeCl(D–X) band is observed from discharges in HCl, Cl_2, and CCl_4 even though XeCl(D) is not formed from Xe($^3P_{2,1}$) atom reactions. The presence of XeCl(D) from the Xe/HCl mixture is especially significant because the available energy from Xe($^3P_{1,2}$) + HCl constrains the XeCl* emission to a very narrow band at 308.0 nm.[3] The short wavelength limit from the Xe/HCl discharge, which could help to identify the XeCl(B) formation step, could not be obtained from the spectrum in Figure 1 because the photomultiplier sensitivity decreased rapidly below 200 nm. Therefore, spectra were acquired with the 0.3-m monochromator and a 150-nm blazed grating plus a VUV photomultiplier tube (EMR-541F) with N_2 flushing of the monochromator; a spectrum is shown in Figure 4. The short wavelength limit from Xe/HCl is 200 nm, corresponding to at least 6.2 eV of available energy. Due to the improved response to the detection system below 300 nm, the oscillations of the spectrum in Figure 4 are more distinct than in Figure 1.

Experiments were done with Cl_2 and HCl (0.2 torr of 1% mixtures) with pulsed dc discharge excitation. The XeCl* emission spectra from the dc discharge (1500 V) were identical, to within the experimental error, with the tesla discharge spectra shown in Figures 1 and 2. The emission intensities were quite strong with that from HCl being only a factor of 2 lower than the emission intensity from Cl_2. Spectra also were taken at three characteristics times from the pulsed discharge in Xe/HCl and Xe/Cl_2 mixtures; (i) the initial buildup of XeCl* intensity following the beginning of the discharge, (ii) the emission while the discharge was on (the intensity oscillates slightly in time during this period), and (iii) the emission from the afterglow after the discharge terminates. It was necessary to have a discharge pulse width of 150 μs to obtain all three regions, otherwise only (i) was observed. There were only minor differences in the XeCl* spectra from the three regions and again, to within experimental uncertainty, the spectra are the same as shown in Figures 1 and 2 for HCl and Cl_2. The decay times of the XeCl* emission intensity from the pulsed discharge are considered in section D.

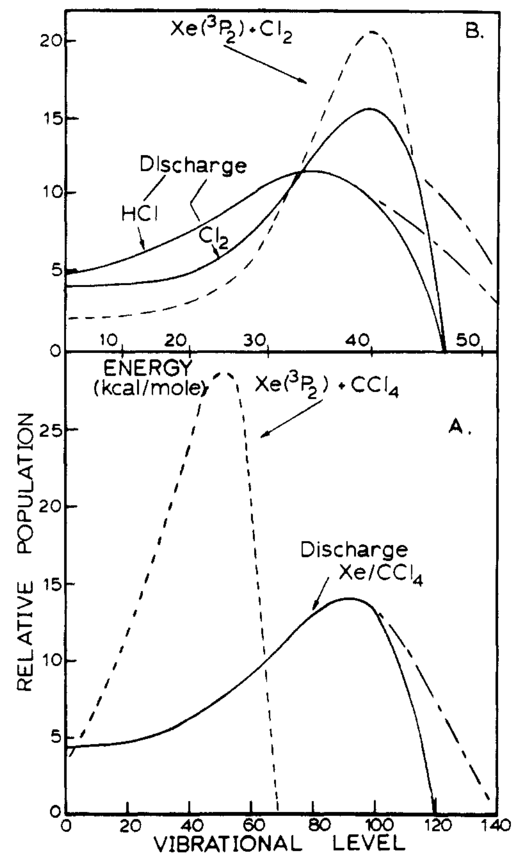

Figure 5. The XeCl(B) vibrational distributions assigned from computer simulation of the XeCl(B–X) spectra shown in Figures 1–3. (A) comparison of distributions from CCl_4/Xe discharge with that from the Xe($^3P_2$) + CCl_4 reaction. (B) distributions from Cl_2/Xe and HCl/Xe discharges, the distribution from Xe($^3P_2$) + Cl_2 is also shown for comparison. The discharge distributions are thought to include the high-energy tails shown by the dashed lines; however, this part of the distribution is not reliable (see text). The remaining parts of the discharge distributions (solid lines) are the sum of a flat component and a linear surprisal component.

Computer simulation of XeCl(B–X) spectra give estimates of the XeCl(B) vibrational distributions.[3b] The high-energy portion of the XeCl(B) vibrational distributions are hard to assign because the potential curves were not well characterized for $v \gtrsim 120$,[3b] and the spectra are too noisy for accurate simulation. When the methods described previously were used,[3b] the distributions shown in Figure 5 were assigned. The high-energy tails of the distributions are shown as dashed lines in Figure 5. The rather broad XeCl(B) vibrational distributions from discharge excitation contrasts with the sharply peaked distributions from the reactions of Xe($^3P_{1,2}$) with CCl_4 and Cl_2.[3,4]

We did not monitor the metastable or resonance atom concentrations in the discharge and cannot specify the relative contribution of the Xe(6s) atom reaction channel to the spectra in Figures 2–4. Some Xe(6s) states must be present as evidenced from the following observations: (i) atomic emission lines which terminate in these levels, (ii) the XeCl* intensities depend upon the reagent with that from Cl_2 being the strongest, which is expected based

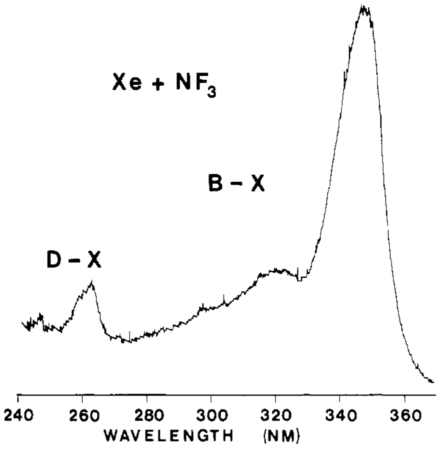

Figure 6. Spectrum from the NF_3/Xe discharge at 0.2-nm resolution: P_{Xe} = 0.85 torr and P_{NF_3} = 0.05 torr. The XeF(B–X) and (D–X) bands are labeled the XeF(C–A) band which extends beyond 380 nm is badly overlapped by Xe lines and is not shown.

TABLE I: Xe($^3P_2$) Quenching Cross Sections and XeX* Formation Branching Fractions

reagent	σ,[a] Å^2	Γ(XeX*)
Cl_2	193	1.0[b]
HCl	119	<0.02[b]
CCl_4	150	0.13[b]
NF_3	23	1.1[c]
C_2F_6		0[c]
BF_3	~56	0[c]
SF_6	75	~0[c]

[a] Reference 2. [b] Reference 3a. [c] Reference 1 and 4a.

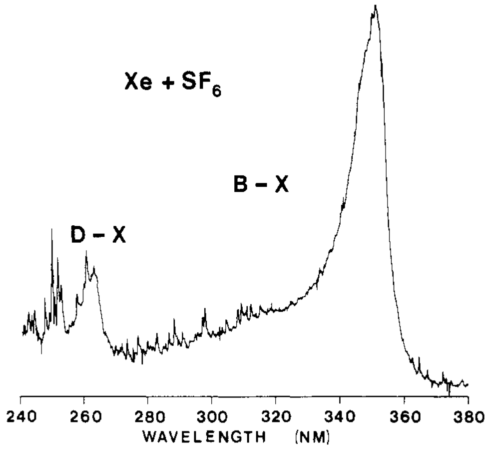

Figure 7. Spectrum from the SF_6/Xe discharge at 0.2-nm resolution: P_{Xe} = 0.46 torr and P_{SF_6} = 0.01 torr. The XeF(B–X) and (D–X) bands are labeled.

on branching fractions for Xe($^3P_{2,1}$) reactions, and (iii) the vibrational distributions from Cl_2 and CCl_4 appear as the Xe($^3P_2$) spectrum[3] plus a broad, higher energy component. On the other hand, the common appearance of the XeCl* spectra from tesla excitation, the high vibrational energy component of the distributions, and the formation of XeCl(D) are not compatible with only Xe($^3P_{2,1}$) atom reactions and suggest another XeCl* formation reaction pathway that is dominant for Xe/HCl and complementary for Xe/CCl_4 and Xe/Cl_2 mixtures. The inclusion of the other two Xe(6s) states, $^3P_0$ and $^1P_1$, with the $^3P_{2,1}$ states would not change this conclusion.

B. Xe + RF. The tesla discharge of Xe/NF_3 mixtures produced the XeF* spectrum shown in Figure 6. The main features are a D–X band at 265 nm and a strong B–X band. The C–A band is overlapped by Xe** lines, which are present above 450 nm (see Figures 1–3). In contrast to the XeCl(B–X) emission observed from the RCl reactions, there is only a single, very shallow oscillation in the XeF(B–X) band. This is partially due to relaxation at the higher pressure used in obtaining the spectrum in Figure 6 and at lower pressure the oscillation is slightly more significant, but the signal-to-noise ratio is much lower and the spectra are not reproduced here. Even at 0.25 torr, however, the XeF* oscillations are less pronounced than those for XeCl*. This is an intrinsic characteristic of XeF(B–X) spectra, which has more widely spaced oscillations than XeCl(B–X) for the same vibrational excitation.[3,11] A tesla discharge of Xe/SF_6 gave the XeF* spectrum shown in Figure 7. The spectrum is very similar to that of Xe/NF_3 and the B–X band does not show any oscillations even at 0.5 torr. The situation with SF_6 is similar to that of the Xe/HCl discharge, i.e., an XeF* spectrum is observed which cannot arise from the reaction of Xe($^3P_2$) or Xe($^3P_1$) with SF_6 (see Table I). Like the chlorine donor systems, the XeF* spectrum from both NF_3 and SF_6 are quite similar, suggesting that a common pathway is forming XeF* in both cases.

Tesla discharges of Xe/C_2F_6 and Xe/BF_3 mixtures gave no XeF* emission for partial pressures of reagent ranging from 0.05 to 0.6 torr. The Xe($^3P_2$) reactions with C_2F_6 and BF_3, which have substantial quenching cross sections (Table I), also have negligible XeF* formation branching fractions. Since the Xe atomic emission intensity appeared to be normal from the Xe/C_2F_6 and Xe/BF_3 discharges, the interactions of these reagents with Xe** and/or Xe^+ must differ in a fundamental way from SF_6 or NF_3.

C. Xe + N_2O. There is some interest in the possibility of a laser based on a transition of XeO. Bischel et al.[7b] reported observing broad-band green emission from XeO in the reaction of Xe** + N_2O where the Xe** was initially formed in the $2p_6$ level via two-photon absorption of KrF (248 nm) laser radiation. We admitted Xe and N_2O into our tesla discharge at pressures up to 1.5 torr and failed to observe XeO emission. The spectra observed consisted of Xe lines and strong NO γ bands.

*D. Time Dependence of Xe** and XeCl Emission.* The time dependence of the Xe** and XeCl(B–X) emission intensities from the tesla flow cell was measured for pure Xe and Xe/HCl or Xe/Cl_2 mixtures. The Xe** emission was observed with a red cutoff filter at 695 nm and with the monochromator set at 823.2 nm, corresponding to the strong $Xe(6p[3/2]_2 \rightarrow 6s[3/2]_2)$ or ($2p_6 - 1s_5$ (or $^3P_2$)) transition. The XeCl(B–X) emission was observed at 306.0 nm. The time dependence of both the Xe** and XeCl(B) emission signals were the same. The waveform at short time intervals (<5 μs) consisted of an intense signal which grew as a series of fast oscillations and decayed with a time constant on the order of 250–500 ns. This result is similar to the observations of McKeever et al.[9a] although our resolution of the very fast oscillations from the discharge was not as good as theirs and reflects the timing of the primary tesla discharge. At longer times the emission intensities decayed with time constants on the order of several microseconds and these are illustrated in Figure 8 for four cases: (a) Xe** from a discharge in Xe alone, (b) Xe** from a discharge in Xe/HCl, (c) XeCl* from a discharge in Xe/HCl, and (d) XeCl* from a discharge in Xe/Cl_2. For all cases the initial peak intensity decays exponentially toward zero. The apparent plateau after the initial pulse decay is due to quantization of the small signal by the transient digitizer. After a time interval of 200 μs, a secondary pulse occurs, consisting of random events which appear to have a temporal character similar to that of the primary discharge emission. On a longer time scale

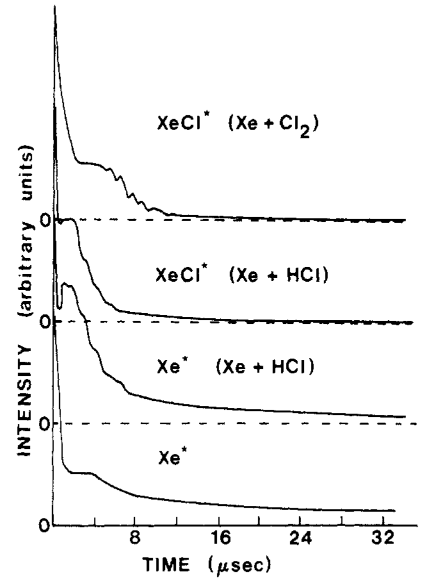

Figure 8. Long-term decay of the emission intensities from the tesla discharge. Four curves are shown vertically displaced: (A) $Xe(2p_6-1s_5)$ from Xe (0.15 torr) alone; (B) $Xe(2p_6-1s_5)$ from Xe (0.15 torr) + HCl (0.01 torr); (C) XeCl(B–X) at 306.0 nm from Xe (0.15 torr) + HCl (0.01 torr); and (D) XeCl(B–X) at 306.0 nm from Xe (0.15 torr) + Cl_2 (0.01 torr).

we observe the 120-Hz oscillation (repetition) in the emission.

The time dependence of the Xe** and XeCl* emission intensities in Xe/HCl mixtures were investigated more completely in the afterglow of the pulsed discharge. In addition to the $Xe(2p_6 - 1s_5)$ transition, a sampling of other Xe(6p, 7p, 8p) transitions were studied. All Xe** states had decay times in the range of 60–100 μs at a Xe pressure of 0.2 torr; the Xe** decay times were relatively independent of Xe pressure from 0.2 to 1 torr. An inverse correlation of decay times of both Xe** and XeCl(B) was found with HCl pressure. For example, at a total pressure of 0.2 torr, the XeCl(B) decay times in 10, 2.5, and 0.5% HCl mixtures were ~3, 15, and 140 μs, respectively. Variation of the Xe pressure from 0.1 to 2 torr for a fixed HCl pressure of 0.2 torr has a small and nonsystematic effect on the XeCl(B) decay times, i.e., the decay time increased ~50% at 0.5 torr and then slowly declined with further increase in Xe pressure. In summary, the decay times of both the Xe** and XeCl* emission intensities in the afterglow of the pulsed discharge are similar. Furthermore, the decay times are in agreement with the long time measurements from the tesla discharge experiments. The Xe** and XeCl* decay times decrease with an increase in HCl concentration, but are relatively invariant to Xe pressure from 0.1 to 1.0 torr.

Discussion

A. XeX Formation Mechanisms in Low-Pressure Discharges.* The three most likely general reaction pathways for XeX* formation in low-pressure electrical discharges are summarized as follows:

$$Xe(6s) + RX \rightarrow XeX^* + R \quad \text{Xe(6s) atom reactions} \tag{1}$$

$$Xe^{**} + RX \rightarrow XeX^* + R \quad \text{Rydberg atom reactions} \tag{2}$$

$$Xe^+ + X^- + M \rightarrow XeX^* + M \quad \text{ionic recombination} \tag{3}$$

The major question is which of the above channels is dominant for a given experimental situation. We cannot a priori rule out any one of these formation processes for the tesla discharge. Depending on the gas mixture and total pressure, the plasma may appear as a glow discharge or a filament discharge. Significant quantitites of both electrons and Xe^+ ions must be present. The Xe** atoms, formed either by electron impact excitation or by Xe^+ + 2e recombination, obviously are present because emission from them is observed. The Xe(6s) levels are generated by electron collisions and by radiative cascade. Before examining reactions 1–3 in further detail, other possible XeX* formation pathways should be eliminated.

Although the $Xe(^3P_2)$ + HCl(v=0) reaction is slightly endothermic for production of XeCl(B), which is consistent with the large quenching cross section but low XeCl* branching ratio (Table I), addition of one or more HCl vibrational quanta (0.37 eV) will make the reaction exothermic. However, four HCl vibrational quanta are required to yield XeCl(D) and even more energy is required to produce the full distribution of Figure 5. The tesla discharge does not significantly heat the tube flow and the HCl molecules are not sufficiently vibrationally excited to account for the observed XeCl* spectrum. An explicit test for the presence of vibrationally excited HCl was made by use of the pulsed dc discharge. For the Xe/HCl mixtures used to study the XeCl* emission, HCl infrared emission could not be observed by a high-sensitivity InSb (Barnes Engineering) detector plus interference filter. In fact HCl infrared emission could not be observed for any discharge conditions with 1–20% HCl mixtures and either He, Ar, or Xe in the 0.1–5-torr pressure range. In contrast strong infrared emission was observed for these same conditions from CO/rare gas mixtures. We conclude, with *confidence*, that vibrationally excited HCl does not explain the XeCl* formation process in the low-pressure discharge.

Another possibility is the reaction of an excited state of the halide molecule with Xe.[8] Most spectra contain the weak Cl_2(E–B) band at 249 nm, due to impurities and/or secondary Cl_2 formation for HCl and CCl_4, showing that excited states of RX are present. However, the Cl_2(E) state, in particular, does not have enough energy (T_e = 7.18 eV)[15] to yield XeCl(D) and there is no evidence of emission from other RX** states. Also, increasing the pressure of the halide reagent at a constant Xe pressure causes the XeX* intensity to decrease, not increase. Finally, the lifetimes of high-lying RX** states normally are ~50 ns, thus radiative cascade rather than collisional quenching should be the dominant loss process under our conditions. Thus, RX** reactions are unlikely to contribute to XeX* excitation in a major way. Nevertheless, for pulsed discharge experiments with HCl/Xe and HBr/Xe mixtures there were indications of XeCl* or XeBr* formation from products generated under long pulse operation. These secondary processes could be formation of Cl_2 (or Cl_2^*) and Br_2 (or Br_2^*) followed by subsequent reaction with $Xe(^3P_2)$ (or Xe). Certainly some care must be exercised regarding chemical composition before, during, and after the discharge.

For reagents (see Table I) that have high branching fractions for XeX* formation upon interaction with Xe(6s), reaction 1 must contribute significantly toward XeX* formation. However, in two important cases, HCl and SF_6, the $Xe(^3P_{2,1})$ atoms yield little or no XeX*, while strong emission is observed from low-pressure discharge excitation. Obviously (1) cannot be responsible for the XeCl*

---

(14) A. P. Vitols and H. J. Oskam, *Phys. Rev. A*, 8, 1860 (1973).

(15) (a) K. P. Huber and G. Herzberg, "Constants of Diatomic Molecules", von Nostrand, New York, 1979. (b) B. Darwent, *Natl. Stand. Ref. Data Ser., Natl. Bur. Stand.*, No. 31 (1970).

TABLE II: Bond Energies and Electron Attachment Data

reagent	D^0-(R-X), eV	EA, eV	AP, eV	principal ion	thermal attachment rate constant, $cm^3\ s^{-1}$
HCl	4.43^a	-0.7^e	0.7^e	Cl^-	$\sim 3 \times 10^{-13\,l}$
Cl_2	2.48^a	2.5^f	0^j	Cl^-	$1.1 \times 10^{-9\,m}$
CCl_4	2.9^b	2.5^g	0^q	Cl^-	$4.1 \times 10^{-7\,m}$
NF_3	2.5^b	>0	$\sim 0^k$	F^-	$2.1 \times 10^{-11\,k}$
C_2F_6	5.5^c		2.1^c	F^-	
BF_3	6.9^b	$<0^h$	10.4^c	F^-	
SF_6	4.0^d	$0.5-0.7^i$	0^n	SF_6^-, SF_5^-	$2.2 \times 10^{-7\,n}$

[a] Reference 15a. [b] Reference 15b. [c] Reference 16. [d] Reference 17. [e] Reference 18. [f] Reference 19. [g] Reference 20. [h] Reference 21. [i] Reference 22. [j] Reference 23. [k] Reference 24. [l] Reference 25. [m] Reference 26. [n] Reference 27.

and XeF* formation from HCl and SF_6. The question of how much of the XeX* emission observed from Cl_2, CCl_4, and NF_3 comes from (1) cannot be answered directly; however, there are two significant points. The XeCl* spectra from all three RCl reagents have similar B–X, D–X, and C–A relative intensities, although the XeCl vibrational distributions do differ (see Figure 5). The XeF* spectra are less distinctive, but the relative B–X and D–X band intensities are the same from both NF_3 and SF_6, and also the B–X envelopes are similar for both. The second point is the higher I(D–X)/I(B–X) ratio from the discharge than from the $Xe(^3P_{2,1})$ atom reactions. The Xe(6s) atom reactions must contribute to XeX* formation for Cl_2, CCl_4, and NF_3 in the tesla discharge, but a second reaction channel yielding higher energy XeX* molecules also must be operative. This second channel is common to all the systems which yield XeX* and makes the major contribution for HCl and SF_6. The most likely possibilities are either (2) or (3) and these are examined in detail below.

B. XeCl Formation by Ion Recombination.* Atomic ionic recombination must be considered rather than molecular recombination because three-body formation of Xe_2^+ is too slow ($k = 2 \times 10^{-31}$ $cm^6\ s^{-1}$)[14] at pressures below 1 torr to generate Xe_2^+. Three-body recombination reactions can be expected to give XeX* with initial vibrational energies near the dissociation limit. However, two-body dissociative recombination may give a lower vibrational distribution.

$$Xe^+ + RX^- \rightarrow XeX^* + R \qquad (4)$$

The intermediate stages of (4) closely resemble the Xe(6s) reaction pathways, which proceed via a Xe^+, RX^- intermediate. The difference is that (4) has higher, IP(Xe) − E(Xe,6s), available energy. An important criterion for ionic recombination is the concentration of X^- or RX^-. Electron affinities, appearance potentials for negative ions, and attachment rate constants are listed in Table II. The reagents which did not give XeF* in the discharge, BF_3 and C_2F_6, do *not* attach low-energy electrons. Harland and Franklin[16] have measured the following branching ratios for electron energies corresponding to the peak in the capture cross section:

$$C_2F_6 \rightarrow F^-:CF_3^-:C_2F_5^- = 100:21:1$$

$$BF_3 \rightarrow F^-:F_2^-:BF_2^- = 1000:20:<1$$

$$NF_3 \rightarrow F^-:NF^-:F_2^-:NF_2^- = 1000:0:5:1.2$$

Because of their high threshold energies, only modest concentrations of F^- might be expected from C_2F_6 and BF_3 in the discharge. Fehsenfeld[27] measured the branching ratio for thermal electron attachment to SF_6 as SF_6^-:SF_5^-:F^- = 200000:1:0 at 20 °C. The SF_6^- is very weakly bound relative to SF_5^- + F and at 200 °C; SF_6^-:SF_5^- is 25:1. The appearance potential for F^- from SF_6 is located at higher electron energies, but the concentration of F^- is always less than that of SF_6^- + SF_5^-.[27] The fact that SF_6 readily attaches thermal electrons yet does not react with $Xe(^3P_2)$ to form XeF* has been associated with the SF_6^- anion, which gives a Xe^+, SF_6^- intermediate that predissociates rather than forms XeX*.[1,4a] Two-body recombination of Xe^+ and SF_6^- presumably would follow the same pathway. The Xe^+ and SF_5^- recombination also would involve an intermediate since SF_5^- is stable and predissociative channels may compete with XeF* formation. Although attachment by CCl_4 gives Cl^- and Cl_2^-, the threshold for Cl^- is ~0 eV while that for Cl_2^- is 2.3 eV[20,26] and two-body dissociation recombination (reaction 4) need not be considered. The above analysis suggests that RX^- ions are unimportant for the systems of interest and that attention can be concentrated on the three-body process.

Flowing afterglow experiments at ~1 torr of He pressure have shown that two-body Xe^+ + Cl^- recombination (mutual neutralization) is slower than ambipolar diffusion;[29] the upper limit for mutual neutralization was $\leq 0.5 \times 10^{-8}$ $cm^3\ s^{-1}$. Atomic ion recombination must be three-body under our experimental conditions. Theoretical treatments[30] for the three-body rate constant give $k \sim 10^{-25}$ $cm^6\ s^{-1}$; experimental measurements are not available. For ion densities between 10^9 and 10^{12} cm^{-3}, the decay time of the three-body process will range between 1 and 10^{-3} s. Wall neutralization is the most serious ion loss mechanism in our discharge experiments and the rate is determined by the diffusion to the wall. The mean diffusion time to reach the wall is given by $\tau_D = \Lambda^2/D_a$ where D_a is the ambipolar diffusion coefficient; $D_a = D_+(1 + T_e/T_g)$ with D^+ the diffusion coefficient for Xe^+ in Xe, T_e the electron temperature, and T_g the bath gas temperature. For T_g = 300 K, $T_e = T_g$, $D_+ = 23/P_{Xe}$ $cm^2\ torr^{-1}\ s^{-1}$,[31] P_{Xe} = 0.2 torr,

---

(16) P. W. Harland and J. L. Franklin, *J. Chem. Phys.*, **61**, 1621 (1974).

(17) T. Kiang and R. N. Zare, *J. Am. Chem. Soc.*, **102**, 4024 (1980).

(18) J. P. Ziesel, I. Nenner, and G. J. Schulz, *J. Chem. Phys.*, **63**, 1943 (1975).

(19) (a) S. Y. Tang, C. B. Leffert, E. W. Rothe, and G. P. Reck, *J. Chem. Phys.*, **62**, 132 (1975); (b) W. A. Chupka, J. Berkowitz, and D. Gutman, *J. Chem. Phys.*, **55**, 2724 (1971).

(20) J. J. DeCorpo and J. L. Franklin, *J. Chem. Phys.*, **54**, 1885 (1971).

(21) (a) S. Y. Tang, E. W. Rothe, and G. P. Reck, *J. Chem. Phys.*, **60**, 4096 (1974); (b) E. W. Rothe, B. P. Mathur, and G. P. Reck, *J. Inorgan. Chem.*, **19**, 829 (1980).

(22) (a) C. B. Leffert, S. Y. Tang, E. W. Rothe, and T. C. Cheng, *J. Chem. Phys.*, **61**, 4929 (1974); (b) R. H. Compton, P. W. Reinhardt, and C. D. Cooper, *J. Chem. Phys.*, **68**, 2023 (1978).

(23) (a) M. V. Kurepa and D. S. Belic, *Chem. Phys. Lett.*, **49**, 608 (1977); (b) W-C. Tam and S. F. Wong, *J. Chem. Phys.*, **68**, 5626 (1978).

(24) (a) G. D. Sides and T. O. Tiernan, *J. Chem. Phys.*, **67**, 2382 (1977). (b) P. J. Chantry, 31st Annual GEC, Buffalo, N.Y., Abstract MA-5, 1978.

(25) (a) L. G. Christophorou, R. N. Compton, and H. W. Dickson, *J. Chem. Phys.*, **48**, 1949 (1968); (b) W. J. Miller and R. K. Gould, *J. Chem. Phys.*, **68**, 3542 (1978).

(26) E. Schultes, A. A. Christodoulides, and R. N. Schindler, *Chem. Phys.*, **8**, 354 (1975).

(27) F. C. Fehsenfeld, *J. Chem. Phys.*, **53**, 2000 (1970).

(28) J. J. Decorpo, D. A. Bafus, and J. L. Franklin, *J. Chem. Phys.*, **54**, 1592 (1971).

(29) M. J. Church and D. Smith, *J. Phys. D*, **11**, 2199 (1978).

(30) (a) M. R. Flannery, "Atomic Processes and Applications", Burke and B. L. Moiseiwitsch, Ed., North-Holland, Amsterdam, 1976, Chapter 12, p 6. (b) M. R. Flannery and T. P. Yang, *J. Chem. Phys.*, **73**, 3239 (1980). (c) P. R. Bates, *Chem. Phys. Lett.*, **75**, 409 (1980).

(31) A. K. Bhattacharya and J. H. Ingold, *J. Appl. Phys.*, **43**, 1535 (1972).

and a diffusion length ($1/\Lambda^2 = [2.4/R]^2 + [\pi/L]^2$) of 0.17 cm, we obtain a diffusion time of 125 μs. Neutralization at the wall is faster than reaction 3 at the low pressure of our experiments, even assuming very optimistic ion densities. The expected kinetics of the ion processes are compared to the time dependence of the XeCl* emission from Xe/HCl discharges in the next paragraph and the ion recombination process is discounted as the major XeX* formation process for HCl and SF_6 under our experimental conditions.

Figure 8 and the data from pulsed discharge experiments show that the Xe* and XeCl* emissions have nearly the same decay times. In pure Xe the decay time of the Xe($2p_6$) level, after the initial 4 μs, was 22 ± 2 μs, which is much longer than the radiative lifetime of the Xe($2p_6$) level, τ_R = 39 ns.[32b] We believe that this long lifetime reflects the time constant for populating the Xe(6p) levels by collisions of electrons with the Xe(6s) atoms. This effect has been observed previously by Sadeghi and Sabbagh.[33] Addition of 0.01 torr of HCl to the discharge strongly quenched the Xe** emission intensity and reduced the Xe($2p_6$) decay time to 14 ± 6 μs. Since the collision time between Xe($2p_6$) and 0.01 torr of HCl is much longer than the Xe($2p_6$) lifetime, this quenching cannot occur via HCl collisions with the Xe(6p) atoms but rather must proceed via quenching of the precursor(s) to the Xe(6p) levels.

The lifetime for XeCl* emission from the Xe/HCl experiment (~10% mixture) was observed to be 1.9 ± 0.2 μs (Figure 8). This is two orders of magnitude faster than the expected decay time if the rate-limiting step was diffusion of the ions to the walls. We thus conclude that (3) is not a dominant process. It should be remembered that the decay times from the pulsed discharge support the decay times of the tesla discharges (Figure 8).

C. XeCl Formation by Rydberg State Reactions.* By process of elimination (2) remains as the important contributing process in addition to the Xe(6s) atom reactions. Can (2) be reconciled to the XeCl* decay times? The XeCl* decay times correlate inversely with HCl pressure but, for continuity, we will use the same value, 1.9 μs, as in the above paragraph. If reaction with HCl determines this decay time, a Xe** + HCl rate constant of 5×10^{-10} $cm^3\ s^{-1}$ is required. However the radiative decay rate of Xe** is much faster[32] than the observed XeCl** decay rate, and the observed decay time probably reflects the Xe** formation steps just as for a pure Xe discharge. The XeCl** decay time given in Figure 8 for a Xe/Cl_2 discharge was 2.7 ± 0.8 μs, which is slightly longer than that from Xe/HCl, despite the larger Cl_2 quenching cross section for removal of Xe($^3P_2$). Two factors may explain this result. The first is that the Xe($^3P_2$) + Cl_2 reaction contributes to direct formation of XeCl* offsetting the decrease in population of the higher Xe excited states. The second is the large dipole moment of HCl, which may lead to faster electron cooling rates than Cl_2, and thereby decrease the production rate of excited Xe** states. We conclude that the XeCl* decay times need not preclude reaction 2 as being an important contributing formation step.

To explain the XeCl(B) vibrational distribution and the high XeCl(D) population, especially from HCl, the Xe** atoms must have ~10.6 eV of energy. This energy corresponds to the Xe(5d, 7s, 7p, etc.) levels, which are 2–3 eV above Xe($^3P_2$). These manifold of levels are just above the 6p manifold and can be expected to be in equilibrium with the Xe(6p) levels (our decay times were measured for $2p_6$) and have very similar time evolution (as actually was observed by recording the decay of the emission from several of these levels in the pulsed dc discharge). The decay time of the XeCl* emission will be related to both the quenching of the Xe($^3P_2$) atoms and the relaxation of the electron temperature to below ~2.5 eV.

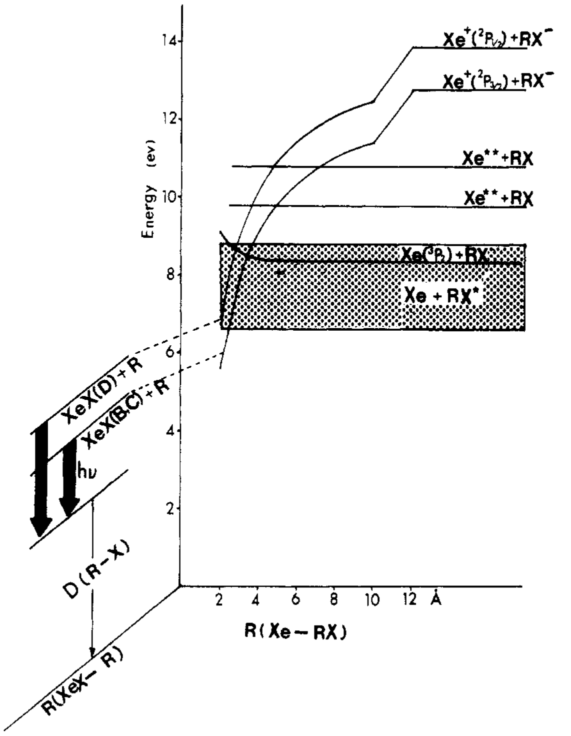

Figure 9. Schematic potential energy diagram for interaction of Xe($^3P_2$) and Xe** (Rydberg) states within a halogen donor of EA = –0.7 eV. Note that, as drawn, the crossing of $V(Xe(^3P_2),RX)$ and $V(Xe^+,RX^-)$ is on the repulsive wall of the Xe($^3P_2$) entrance channel. However, the crossing with the $V(Xe^{**},RX)$ is on the flat part of the entrance channel. The upper Xe** potential denotes the Rydberg states with a $Xe^+(^2P_{1/2})$ core; the lower denotes a $Xe^+(^2P_{3/2})$ ion core. The heavily dotted region denotes the high density of RX* electronically excited states, which will extend to the ionization energy of RX.

The most difficult observation to explain by the Rydberg atom reaction mechanism is the surprisingly strong emission intensity from the SF_6 and HCl (or HBr) discharges.[34] The radiative lifetime for states in the energy range of the Xe(7p) manifold are 0.15–0.30 μs.[32] For an assumed quenching rate constant of 1×10^{-9} $cm^3\ s^{-1}$, the collisional quenching lifetime for P_{RX} = 0.02 torr is ~1.5 μs, and 9–17% of these Xe** states will be converted to XeX*. Although the radiative lifetimes are longer and the quenching rate constants are larger for very high energy Rydberg states, the interaction mechanism with halogen-containing molecules changes and attachment (for SF_6) or dissociative attachment (for CCl_4) of electrons becomes the dominant product channel, at least for Xe** ($n \simeq 20$).[35,36] With regard to XeX* formation by reactive quenching, it seems that attention should be given to experimental characterization of the lower energy Rydberg states.

---

[32] (a) H. Horiguchi, R. S. F. Chang, and D. W. Setser, *J. Chem. Phys.*, **75**, 1207 (1981). (b) M. Aymar and M. Coulombe, *At. Data Nucl. Data Tables*, **21**, 537 (1978).

[33] N. Sadeghi and J. Sabbagh, *Phys. Rev. A.*, **16**, 2336 (1977).

[34] J. K. Ku, unpublished work. The intensity of the XeBr* emission from Xe/HBr mixtures in the pulsed discharge is comparable to that from XeCl* from Xe/HCl mixtures. However, no XeF* emission was observed from pulsed discharge excitation of Xe/HF mixtures.

[35] (a) R. F. Stebbings, C. J. Latimer, W. P. West, F. B. Dunning, and T. B Cook, *Phys. Rev. A*, **12**, 1453 (1975); (b) F. G. Kellert, K. A. Smith, R. F. Rundel, F. B. Dunning, and R. F. Stebbings, *J. Chem. Phys.*, **72**, 3179 (1980); (c) G. W. Foltz, C. J. Latimer, G. F. Hildebrandt, F. G. Kellert, K. A. Smith, W. P. West, F. B. Dunning, and R. F. Stebbings, *ibid.*, **67**, 1352 (1977).

[36] I. Dimicoli and R. Botter, *J. Chem.* Phys. **74**, 2355 (1981).

Summary

Low-pressure experiments with tesla and pulsed discharges have demonstrated that XeCl* or XeF* emission can be obseved readily from mixtures of Xe and halogen-containing reagents, even with reagents which do not yield XeCl* or XeF* by reaction with Xe($^3P_{2,1}$) atoms. Based primarily upon the time dependence of the emission intensities, the ion recombination mechanism was excluded at the principal formation process. We conclude that Xe** states above the Xe(6s) manifold must react with many halogen donors to yield XeX*. Based upon the XeCl(B) vibrational distribution from HCl, the Xe** states may be 2-3 eV above the Xe(6s) levels. The reactive quenching of Xe** atoms but not Xe(6s) atoms can be rationalized by the schematic potential diagram shown in Figure 9. For reagents with negative EA, such as HCl, the intersection of the V(Xe(6s),HCl) and V(Xe$^+$,HCl$^-$) diabatic potentials occurs at short range and possibly on the repulsive wall of V(Xe(6s),HCl). Thus, XeX* formation from the curve-crossing pathway does not compete with other types of quenching mechanisms. However, the V(Xe**,RX) + V(Xe$^+$,RX$^-$) curve crossing will occur at distances such that the interactions are strong,[37b] and transfer to the ion pair potential with subsequent efficient XeX* formation is expected. In discharge experiments Xe** states with both the Xe$^+$($^2P_{3/2}$) and the Xe$^+$($^2P_{1/2}$) core will be present. The Xe** states with the Xe$^+$($^2P_{1/2}$) core naturally correlate to XeX(D),[38] as shown in Figure 9. Both XeX(C) and XeX(B) are formed from Xe** states with the Xe$^+$($^2P_{3/2}$) core since the entrance channel splits into A′ and A″ symmetry in C_s geometry (the Rydberg electron is being ignored) and these correlate to XeX (B and C) states. Thus, the observed XeX* electronic state product distribution can be rationalized in terms of the properties of the Xe** Rydberg states and the covalent-ionic electron-transfer mechanism.[4a] The scheme shown in Figure 9 does not apply to SF$_6$ since EA(SF$_6$) = 0.6 eV. Perhaps the additional energy of Xe**, relative to Xe(6s), results in XeX* formation before the Xe$^+$, SF$_6^-$ complex predissociates.

There are, at least, two other questions involving state-to-state kinetics of interest to XeCl* formation with HCl as the donor molecule. Although we concluded that vibrationally excited HCl was not important in our experiments, the role of HCl vibrational excitation for other experimental conditions is still the subject of debate. Using an HCl laser, Chang[39] has studied Xe($^3P_2$) + HCl(v=1) and claimed an enhanced branching fraction (relative to HCl(v=0)) for XeCl* formation. The enhanced branching fraction probably is insufficient to make the reaction important for the XeCl laser medium. Despite the increase in the dissociative attachment cross section of HCl with increasing temperature[40] (which is associated with HCl vibrational excitation) Rokni[41] has argued that HCl vibrational excitation has no major role in the ion recombination pathway[12] for XeCl* formation in the laser medium. The second question is the possibility of two-body mutual neutralization or predissociation of XeCl* formed by three-body combination of Xe$^+$ and Cl$^-$. If they occur, both are a consequence of interaction of the V(Xe$^+$,Cl$^-$) and V(Xe*,Cl) diabatic potentials. The diabatic curves cross at long range (~100 Å) and the curve crossing probability estimated from the correlation of H_{12} with crossing distance[37b] predicts a vanishingly small neutralization rate constant. However, the thermal neutralization rate constants for alkali metal ion + halogen ions do not follow the theoretical prediction very closely,[37c] so some reservation should be maintained until experimental tests are made. Church and Smith's upper limit value of 0.5 × 10^{-8} cm^3 s^{-1} for Xe$^+$ + Cl$^-$ mutual neutralization is not very restrictive for situations in which diffusive loss of ions is slow. A fully allowed mutual neutralization reaction (such as Cl$_2^+$ + Cl$^-$)[29] has a rate constant of 5 × 10^{-8} cm^3 s^{-1}. If Xe($^3P_2$) atoms are formed by either predissociation[42] of XeCl* molecules generated by three-body ion recombination or by two-body mutual neutralization, then the branching fraction for Xe($^3P_2$) + HCl(v) and the reactive quenching of Xe** + HCl may become important practical questions for the XeCl laser, as well as interesting questions of state-to-state chemistry.

Acknowledgment. This work was supported by the U.S. Department of Energy (DE-AC02-80ET33068). We thank Dr. Nader Sadeghi (Université de Grenoble) for assistance with the pulsed discharge experiments and for a critical reading of the manuscript. We also thank Mr. Trecil Dreiling for doing the computer simulation of the XeCl(B–X) spectra, which gave the distributions shown in Figure 5.

---

[37] (a) R. E. Olson, J. R. Petersen, and J. T. Moseley, *J. Chem. Phys.*, **53**, 3391 (1970); (b) R. E. Olson, F. T. Smith, and E. Bauer, *Appl. Opt.*, **10**, 1848 (1971); (c) R. K. Ianev and Z. M. Radulovic, *J. Chem. Phys.*, **67**, 2856 (1977).

[38] M. F. Golde and R. A. Poletti, *Chem. Phys. Lett.*, **80**, 23 (1981). Professor Golde has observed a propensity for ArCl(B,C) and ArCl(D) formation from reactions of Ar($^3P_2$) and Ar($^3P_0$) atoms, respectively, with Cl$_2$.

[39] R. S. F. Chang, *J. Appl. Phys.*, submitted for publication.

[40] M. Allan and S. F. Wong, *J. Chem. Phys.*, 74, 1687 (1981).

[41] M. Rokni, *Appl. Phys. Lett.*, **39**, 319 (1981).

[42] T. D. Dreiling and D. W. Setser, *J. Chem. Soc., Faraday Trans. 2*, submitted for publication. Predissociation of ArCl*, KrBr*, and KrI* molecules formed by reactive quenching is commonly observed. However, the predissociation gives excited halogen atoms in these cases. In preliminary work apparent formation of Xe($^3P_2$) was observed from He flowing afterglow experiments in which Xe$^+$ and Cl$^-$ ions were simultaneously present; mutual neutralization or three-body recombination are possible explanations.